JACS Au
AN OPEN ACCESS JOURNAL OF THE AMERICAN CHEMICAL SOCIETY

pubs.acs.org/jacsau
Article

Importance of Polar Effects in Halogen-Atom Transfer from Alkyl Iodides to α-Aminoalkyl Radicals. A Kinetic and Computational Evaluation of the Role of Structural and Medium Effects

Jacopo Mancini,[#] Chiara Stavagna,[#] Francesco Pileri, Giovanni Lonardi, Enrique M. Arpa, Marco Galeotti, Sergio Sisti, Fabio Juliá, Michela Salamone,* Daniele Leonori,* and Massimo Bietti*

Cite This: JACS Au 2026, 6, 103−112

Read Online

ACCESS | Metrics & More | Article Recommendations | Supporting Information

ABSTRACT: α-Aminoalkyl radicals have emerged as practical halogen-atom transfer (XAT) agents, enabling the formation of carbon radicals from unactivated alkyl and aryl halides under mild conditions. A recent study correctly revised some of the XAT rate constants for these radicals downward, prompting broad mechanistic conclusions that contradict the key importance of polar effects and challenge the XAT reactivity for α-aminobenzyl radicals. Herein we report a comprehensive kinetic and computational analysis of XAT reactions of α-aminoalkyl and α-aminobenzyl radicals with alkyl iodides under both thermal and photochemical conditions. Laser flash photolysis experiments reveal a clear structure−reactivity relationship shaped by polar and steric effects, which is well supported by the computational results. These findings reaffirm the key importance of the nucleophilic character of α-aminoalkyl radicals in providing significant transition state stabilization to XAT processes. This confirms the prominent role played by polar effects in these reactions and the possibility for reactivity tuning using α-aminobenzyl radicals.

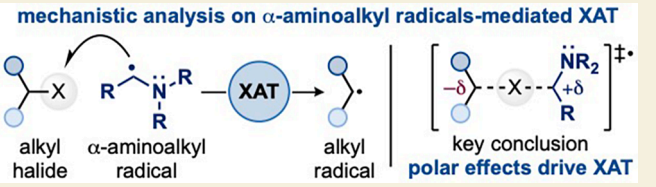

KEYWORDS: *halogen-atom transfer, α-aminoalkyl radicals, polar effects, medium effects, radical reactivity*

INTRODUCTION

Alkyl halides are foundational building blocks in radical chemistry, with extensive use in C−C and C−heteroatom (e.g., F, N, or O) bond formation.[1,2] These compounds are broadly commercially available or can be easily prepared from commonly accessible substrates such as alcohols, alkenes, and alkanes through Appel reaction, hydrohalogenation, or halogenation via hydrogen-atom transfer (HAT).[3−5] Among the various strategies available for converting alkyl halides into alkyl radicals, halogen-atom transfer (XAT) has emerged as being particularly attractive. In contrast to direct photochemical bond homolysis and reductive single-electron transfer (SET),[6−8] XAT avoids the use of high-energy irradiation and strong reductants. As a result, it often provides improved chemoselectivity, broad functional group tolerance, and compatibility for integration with metal catalysis.[9−11]

The driving force for XAT is rooted in thermodynamic principles, specifically the formation of strong bonds between the halogen atom and the abstracting species (Y•) (Scheme 1a).[12] By employing abstractors leading to strong Y−X bonds, the process becomes facile.[13] XAT processes proceed through well-defined, colinear transition states involving the alkyl group, the halogen atom, and the abstractor. Charge separation within this geometry is governed by the electronic features of the halogen, which polarizes the C(sp^3)−X bond. These polar effects manifest as partial negative ($-\delta$) and positive ($+\delta$) charge development on the incipient (R•) and abstracting (Y•) radicals and have been widely discussed and utilized to explain transition state stabilization that enhances reaction kinetics.[14−16] Excellent species that comply with both enthalpic and polar considerations for XAT are Sn- and Si-radicals owing to their high Sn/Si−X BDEs and ability to stabilize positive charge build-up.[17,18] Despite their unquestioned applicability and utility, tin and silicon reagents provide some drawbacks, mostly based on toxicity, cost, and high molecular weight.[19,20]

Among the available XAT mediators, α-aminoalkyl radicals (**B**) have recently emerged as convenient and sustainable alternatives, with growing applications for generating alkyl and aryl radicals from the corresponding iodides and bromides (Scheme 1b).[21−24] These species can be readily accessed from widely available alkyl amine precursors (**A**), either via HAT to electrophilic radicals or through a stepwise process involving oxidative SET followed by deprotonation.[25−27] These reactive open-shell intermediates were designed by considering both enthalpic and polar effects. Although from a thermodynamic

Received: July 24, 2025
Revised: September 29, 2025
Accepted: September 29, 2025
Published: December 12, 2025

Scheme 1. (a) Mechanistic Analysis of XAT Processes on the Basis of Enthalpic and Polar Considerations and (b) XAT Reactivity of α-Aminoalkyl Radicals[a]

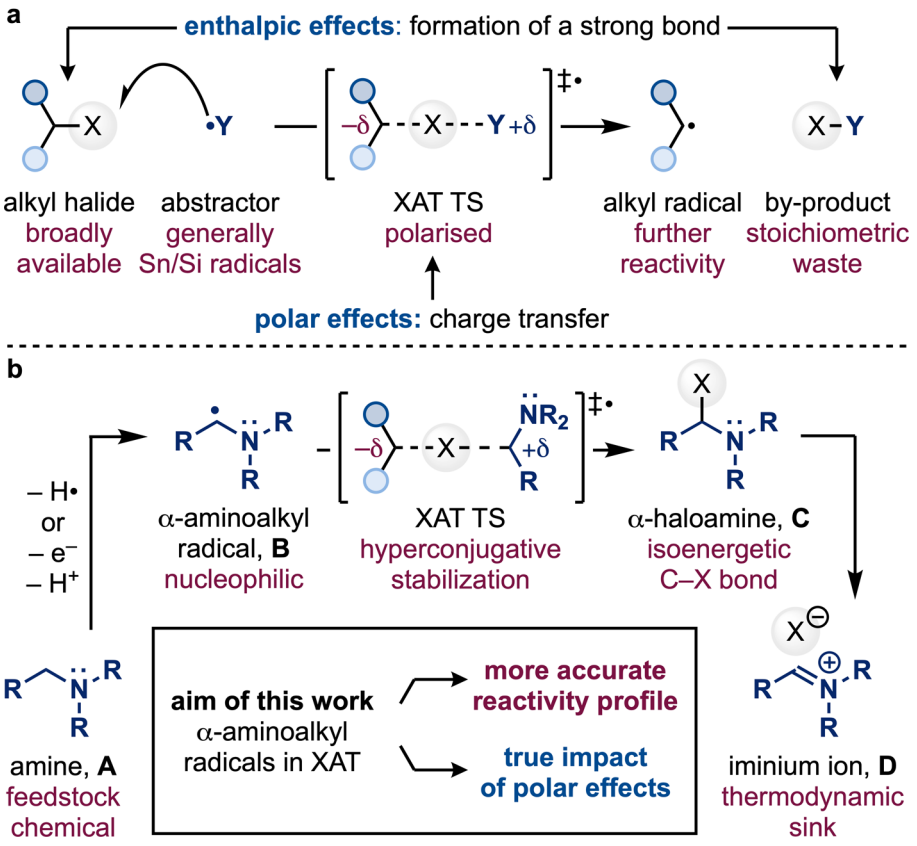

[a]The current work provides an accurate description of their reactivity and the impact of polar effects.

standpoint the similar C(sp^3)–X BDEs of the parent halide and the resulting α-haloamine (**C**) might appear to be an energetic limitation, the rapid and irreversible fragmentation of the α-haloamine into an iminium halide salt (**D**) provides the necessary driving force for the overall transformation. Moreover, the nucleophilic nature of α-aminoalkyl radicals[28] ought to facilitate stabilization of the developing positive charge in the XAT transition state through hyperconjugation with the nitrogen lone pair, thereby promoting efficient charge separation.

Despite this surge in interest, kinetic studies on XAT reactions promoted by α-aminoalkyl radicals are extremely scarce, with only a handful of rate constants currently available. An extensive collection of XAT rate constants would be valuable because it can provide information about the factors that govern XAT reactivity, translating into a quantitative framework for a more systematic application of these reactions in synthetic settings.

The XAT reactivity of α-aminoalkyl radicals with alkyl iodides was initially kinetically measured using an indirect method by means of laser flash photolysis (LFP), using a methyl viologen radical cation as a spectroscopic probe. Under these conditions, a rate constant k_{XAT} = 3.6 × 10^8 M^{-1} s^{-1} at room temperature was derived for the reaction between the α-aminoalkyl radical generated from Et_3N and cyclohexyl iodide (Cy–I), thus putting these systems at a reactivity position slightly below Sn radicals (k_{XAT} > 10^9 M^{-1} s^{-1} at room temperature).[17,29] More recently, to better evaluate the impact of both amine and alkyl iodide structures on these processes, we decided to perform a detailed analysis using a direct method based on transient absorption spectroscopy, following the decay of the α-aminoalkyl radical UV band.[25,30,31] This analysis demonstrated that the indirect method had overestimated the XAT reactivity which, for the same reaction, was more precisely measured as k_{XAT} = 4.49 × 10^6 M^{-1} s^{-1} (vide infra). During the execution of our work, a separate study by Guo and co-workers exploited a powerful time-resolved EPR (TREPR) technique capable of measuring bimolecular rate constants to a cutoff of approximately 10^3 M^{-1} s^{-1}.[32] This method was used to remeasure the rate constant for the same and other XAT reactions, providing a revised and lower k_{XAT} value, which is in line with our ongoing work. However, as part of this study, the authors questioned the reactivity of α-aminobenzyl radicals and the broader mechanistic conclusions concerning the importance of polar effects in XAT processes. In this work, we re-evaluate the mechanistic basis through detailed time-resolved kinetic studies, control experiments, and computational studies to provide a refined, experimentally supported picture of these transformations that confirms the XAT reactivity of α-aminobenzyl radicals and the crucial importance of polar effects in these reactions.

RESULTS AND DISCUSSION

Generation and Characterization of α-Aminoalkyl and α-Aminobenzyl Radicals

α-Aminoalkyl and α-aminobenzyl radicals used in this study were generated via HAT from the α-C(sp^3)–H bonds of the corresponding amine precursors **A1**–**A9** to the cumyloxyl

https://doi.org/10.1021/jacsau.5c00920
JACS Au 2026, 6, 103–112

Table 1. Second-Order Rate Constants (k_{HAT})[a] for the Reaction of CumylO• with Different Amines and Computational Characterization of the Resulting α-Aminoalkyl and α-Aminobenzyl Radicals[d]

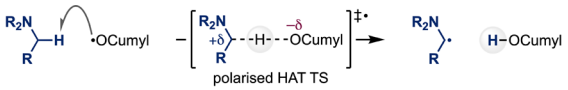

entry	amine	k_{HAT} (M^{-1} s^{-1}) in CH_3CN	k_{HAT} (M^{-1} s^{-1}) in DMSO	α-aminoalkyl/benzyl radical	IP (eV)	*N* (eV)
1	Et_3N **A1**	$2.19 \pm 0.05 \times 10^{8}$[a]	$2.54 \pm 0.04 \times 10^{8}$	Me, NEt_2 **B1**	3.61	10.90
2	Pr_3N **A2**	$2.3 \pm 0.1 \times 10^{8}$	$2.2 \pm 0.1 \times 10^{8}$	Me, NPr_2 **B2**	3.62	10.99
3	$(i\text{-}Bu)_3N$ **A3**	$1.27 \pm 0.02 \times 10^{8}$[a]	$1.29 \pm 0.08 \times 10^{8}$	Me, Me, $N(i\text{-}Bu)_2$ **B3**	3.70	10.94
4	Bn_3N **A4**	4.2×10^{7}[b]	–	Ph, NBn_2 **B4**	3.85	10.91
5	Pr_2NH **A5**	$1.01 \pm 0.03 \times 10^{8}$[a]	$1.35 \pm 0.04 \times 10^{8}$	Me, NHPr **B5**	3.82	10.76
6	Cy_2NH **A6**	$3.23 \pm 0.04 \times 10^{7}$	$4.8 \pm 0.1 \times 10^{7}$	NHCy **B6**	3.78	10.80
7	Bn_2NH **A7**	$3.75 \pm 0.05 \times 10^{7}$[a]	$5.6 \pm 0.1 \times 10^{7}$	Ph, NHBn **B7**	3.97	10.77
8	$CyNH_2$ **A8**	$2.1 \pm 0.1 \times 10^{7}$[c]	$2.83 \pm 0.03 \times 10^{7}$	NH_2 **B8**	3.97	10.60
9	$BnNH_2$ **A9**	$1.8 \pm 0.1 \times 10^{7}$[a]	$2.0 \pm 0.1 \times 10^{7}$	Ph, NH_2 **B9**	4.03	10.71

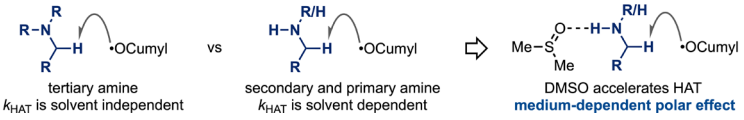

[a]Value obtained from the literature.[34] [b]The overlap between the absorption bands of CumylO• and of the α-aminobenzyl radical formed following HAT from **A4** prevented the determination of k_{HAT}. The given value refers to the reaction of the *t*-BuO• and has been determined employing an indirect method.[39] [c]Value obtained from the literature.[40] [d]All rate constants are the average of at least two determinations.

radical (CumylO•).[33,34] Second-order rate constants (k_{HAT}) for HAT from the amine precursors to this radical, measured in a CH_3CN solution at 25 °C, are available in the literature (Table 1). However, since most of the XAT rate constants in this study were measured in DMSO (vide infra), the corresponding k_{HAT} values were also determined in this solvent. For this purpose, CumylO• was generated by 355 nm laser flash photolysis (LFP) of Ar-saturated DMSO solutions (T = 25 °C), containing 1.0 M $(CumylO)_2$.[35] The k_{HAT} values were obtained by monitoring the decay of CumylO• at its visible absorption maximum (λ_{max} = 490 nm) as a function of the amine concentration. Excellent linear relationships were obtained from the observed rate constants (k_{obs}) vs [amine] plots, and k_{HAT} values were derived from the slope of these plots.

Polarity matching between the electrophilic CumylO• and the hydridic nature of the amine α-C(sp^3)−H bonds ensures relatively fast HAT processes, with k_{HAT} values ranging between 2.0×10^{7} and 2.5×10^{8} M^{-1} s^{-1}, depending on amine structure. No significant increase in k_{HAT} was observed for tertiary amines **A1**−**A3** when switching from CH_3CN to DMSO (entries 1−3). In contrast, k_{HAT} values for secondary (**A5**−**A7**) and primary (**A8**−**A9**) amines increased by up to 50% in DMSO (entries 5−9). This behavior is attributed to the stronger H-bond acceptor ability of this solvent,[36] that by engaging in H-bonding with the amine NH group increases electron density at the α-C(sp^3)−H bonds and enhances HAT reactivity. This effect highlights the importance of medium-dependent polar effects in HAT reactions.[37]

The properties of the resulting α-aminoalkyl and α-aminobenzyl radicals (**B1**−**B9**) were evaluated computationally by determining their ionization potential (IP) and nucleophilicity index (*N*).[38] The results displayed in Table 1 show that all of the radicals examined exhibit comparable nucleophilic character.

XAT Rate Constants: General Considerations

The observed rate constants (k_{obs}) for the reaction of α-aminoalkyl and α-aminobenzyl radicals with the different alkyl iodides (R−I) have been obtained by following the decay of the radical UV or visible absorption band as a function of substrate concentration. The decay of α-aminoalkyl radicals (**B1**−**B3**, **B5**, **B6**, and **B8**) was followed by monitoring their absorption bands around λ = 360 nm,[29,30] while the α-

https://doi.org/10.1021/jacsau.5c00920
JACS Au 2026, 6, 103−112

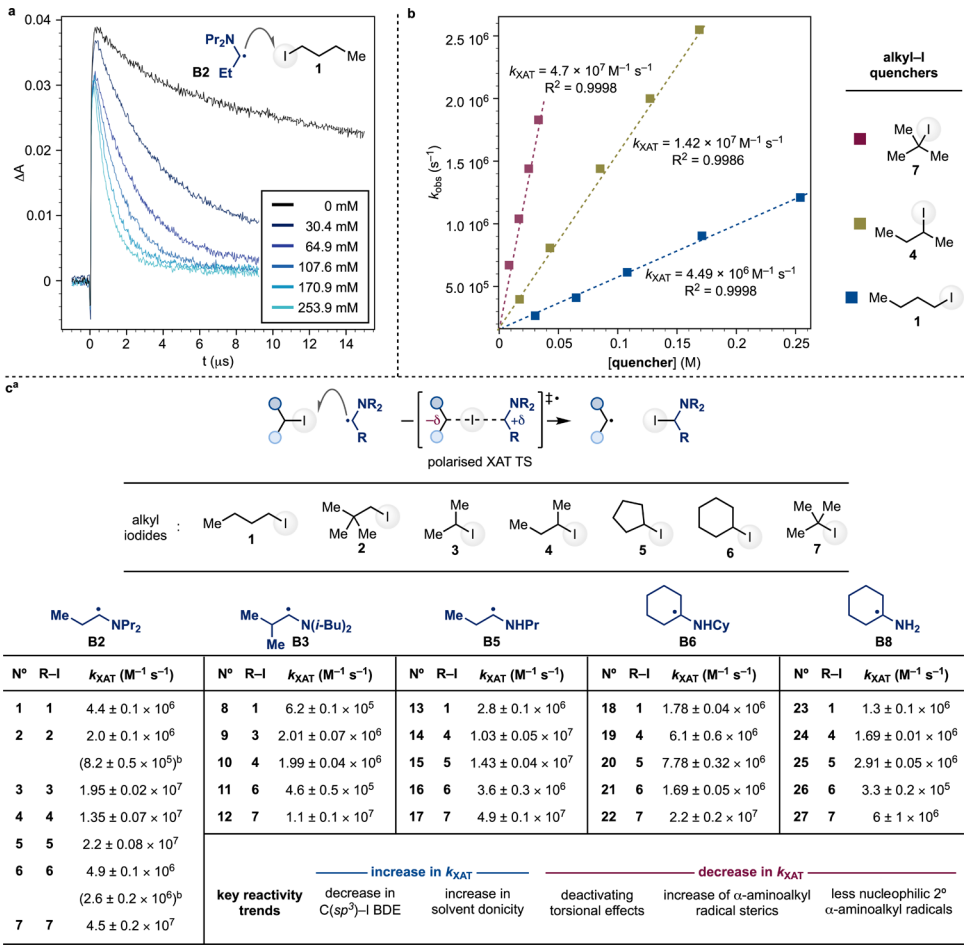

N°	R–I	k_{XAT} (M^{-1} s^{-1})	N°	R–I	k_{XAT} (M^{-1} s^{-1})	N°	R–I	k_{XAT} (M^{-1} s^{-1})	N°	R–I	k_{XAT} (M^{-1} s^{-1})	N°	R–I	k_{XAT} (M^{-1} s^{-1})
1	1	$4.4 \pm 0.1 \times 10^6$	8	1	$6.2 \pm 0.1 \times 10^5$	13	1	$2.8 \pm 0.1 \times 10^6$	18	1	$1.78 \pm 0.04 \times 10^6$	23	1	$1.3 \pm 0.1 \times 10^6$
2	2	$2.0 \pm 0.1 \times 10^6$	9	3	$2.01 \pm 0.07 \times 10^6$	14	4	$1.03 \pm 0.05 \times 10^7$	19	4	$6.1 \pm 0.6 \times 10^6$	24	4	$1.69 \pm 0.01 \times 10^6$
		$(8.2 \pm 0.5 \times 10^5)$[b]	10	4	$1.99 \pm 0.04 \times 10^6$	15	5	$1.43 \pm 0.04 \times 10^7$	20	5	$7.78 \pm 0.32 \times 10^6$	25	5	$2.91 \pm 0.05 \times 10^6$
3	3	$1.95 \pm 0.02 \times 10^7$	11	6	$4.6 \pm 0.5 \times 10^5$	16	6	$3.6 \pm 0.3 \times 10^6$	21	6	$1.69 \pm 0.05 \times 10^6$	26	6	$3.3 \pm 0.2 \times 10^5$
4	4	$1.35 \pm 0.07 \times 10^7$	12	7	$1.1 \pm 0.1 \times 10^7$	17	7	$4.9 \pm 0.1 \times 10^7$	22	7	$2.2 \pm 0.2 \times 10^7$	27	7	$6 \pm 1 \times 10^6$
5	5	$2.2 \pm 0.08 \times 10^7$												
6	6	$4.9 \pm 0.1 \times 10^6$												
		$(2.6 \pm 0.2 \times 10^6)$[b]												
7	7	$4.5 \pm 0.2 \times 10^7$												

Figure 1. (a) Decay traces monitored at λ = 360 nm for the reaction of radical **B2** with **1**. (b) Plots of the observed rate constant (k_{obs}) against [R–I] for the reactions of radical **B2** with **1** (blue squares), **4** (yellow squares), and **7** (red squares). (c) Second-order rate constants (k_{XAT}) for the reaction of the α-aminoalkyl and α-aminobenzyl radicals with different alkyl iodides. [a]Measured in argon-saturated DMSO solution containing 1.0 M $(CumylO)_2$ and 0.05–0.10 M amine at T = 25 °C. The k_{XAT} values have been determined from the slope of the k_{obs} vs [R–I] plots, where k_{obs} values have been measured following the decay of the α-aminoalkyl radicals at λ = 360 nm (Figures S4–S19, S21–S31, and S33–S37) or α-aminobenzyl radicals at λ = 440–480 nm (Figures S20, S31, and S38). Average of at least two determinations. [b]Measured in a CH_3CN solution.

aminobenzyl radicals were monitored via their visible absorption bands centered at λ = 440 (**B9**), 460 (**B7**), and 480 (**B4**) nm,[25] respectively (see Figures S39–S41 in the SI). When the k_{obs} values have been plotted against [R–I], excellent linear relationships were obtained, and the second-order XAT rate constants (k_{XAT}) were derived from the slope of these plots. The k_{XAT} values thus obtained for the reactions of radicals **B2**, **B3**, **B5**, **B6**, and **B8** are collected in Figure 1c. Those for the reactions of radicals **B1**, **B7**, and **B9** are displayed in the Supporting Information (SI).

XAT Rate Constants and Substrate Effects for α-Aminoalkyl Radicals

Initial experiments were carried out in CH_3CN employing **A1** and **A2** as the α-aminoalkyl radical **B1** and **B2** precursors. However, because of the greater intrinsic stability displayed by these radicals in DMSO, this solvent was selected for k_{XAT} determination. To measure k_{XAT} values, the formation of the α-aminoalkyl (or α-aminobenzyl) radical via HAT to CumylO• must be significantly faster than its decay by XAT from the alkyl iodide. Because the k_{HAT} values displayed in Table 1 range between 2.0×10^7 and 2.5×10^8 M^{-1} s^{-1}, concentrations of the amine precursors ≥ 0.05 M have been employed in all the experiments, ensuring sufficiently fast rates of formation (vide infra).

As an example, Figure 1a displays the increase in the rate of decay of **B2** upon addition of increasing amounts of **1** from where the various k_{obs} values can be obtained. Figure 1b shows the k_{obs} vs [R–I] plots for the reactions of radical **B2** with Bu–I (**1**), *s*-Bu–I (**4**), and *t*-Bu–I (**7**), in DMSO solution at T = 25 °C. Additional plots for the reactions of other alkyl iodides with both α-aminoalkyl and α-aminobenzyl radicals are available in the SI (Figures S4–S38).

To discuss substrate structural effects on reactivity, k_{XAT} values for the reaction of a single radical with different alkyl iodides have been initially compared. Taking **B2** as a reference XAT reagent, the results displayed in Figure 1c highlight the existence of pronounced structural effects on reactivity, with a 10- and 22-fold increase in k_{XAT} observed going from primary **1** and neopentyl **2** to tertiary alkyl iodide **7**, respectively (compare entries 1 and 2 with entry 7). The k_{XAT} values increase in the order primary < secondary < tertiary in line with the corresponding decrease in C(sp^3)–I BDEs along the series (BDE = 56.6, 56.1, and 54.3 kcal mol^{-1}, for representative alkyl iodides such as Pr–I, *i*-Pr–I, and *t*-Bu–I, respectively),[41] indicating that bond strengths dominate over

https://doi.org/10.1021/jacsau.5c00920
JACS Au 2026, 6, 103–112

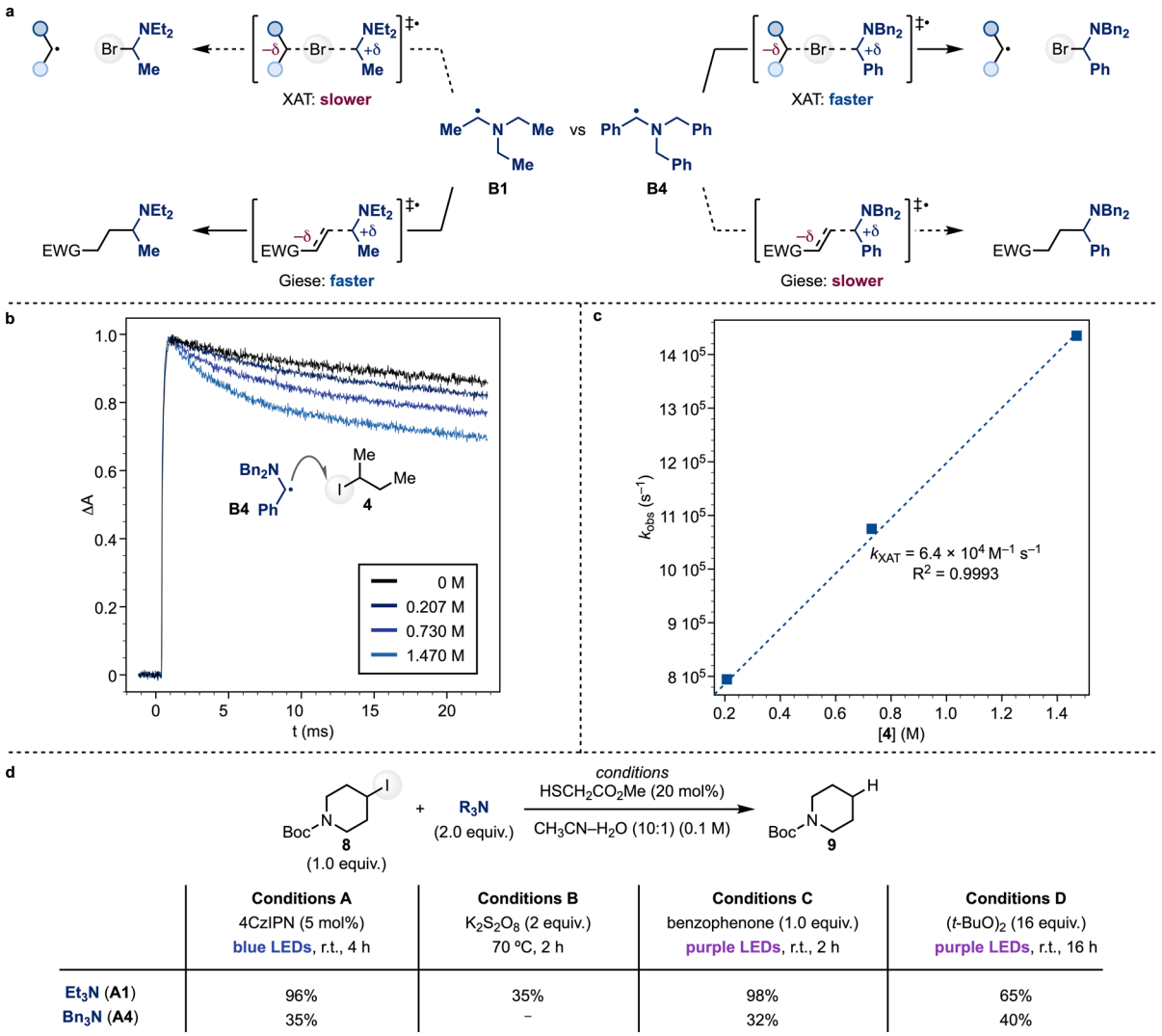

	Conditions A 4CzIPN (5 mol%) blue LEDs, r.t., 4 h	Conditions B $K_2S_2O_8$ (2 equiv.) 70 °C, 2 h	Conditions C benzophenone (1.0 equiv.) purple LEDs, r.t., 2 h	Conditions D (*t*-BuO)$_2$ (16 equiv.) purple LEDs, r.t., 16 h
Et_3N (**A1**)	96%	35%	98%	65%
Bn_3N (**A4**)	35%	–	32%	40%

Figure 2. (a) Different reactivities of α-aminoalkyl and α-aminobenzyl radicals **B1** and **B4** with alkyl bromides (XAT) and electron-poor olefins (Giese addition). (b) Decay traces monitored at λ = 480 nm for the reaction of radical **B4** with **4**. (c) Plots of the observed rate constant (k_{obs}) against [substrate] for the reaction of radical **B4** with **4**. (d) Radical dehalogenation of **8** using amines **A1** and **A4**.

steric effects (compare entries 1, 3, or 4 and 7). Analysis of the kinetic data uncovers nevertheless a small role played by steric effects, evidenced by the 2.2-fold decrease in k_{XAT} measured going from primary **1** to neopentyl iodide **2** (compare entries 1 and 2). It is also interesting to compare the results obtained for secondary iodides, where similar k_{XAT} values have been measured for **3**, **4**, and cyclopentyl iodide **5** (entries 3−5), whereas a sizable decrease in reactivity (4.5-fold with respect to **5**) has been observed for cyclohexyl iodide **6** (entry 6). At present, we do not have a clear-cut explanation for this behavior, which may be tentatively rationalized on the basis of deactivating torsional effects. These effects have been observed to be particularly important in HAT reactions from cyclohexane derivatives and might also be relevant in XAT settings.[42] It is also worth noting the ∼2-fold decrease in k_{XAT} measured for the reactions of both **2** and **6** (entries 2 and 6), going from DMSO to CH_3CN, a behavior that could reflect the greater donicity of the former solvent[43] that can better accommodate polar effects by stabilizing positive charge development in the XAT transition state.

Very similar k_{XAT} values have been measured for the corresponding reactions of α-aminoalkyl radical **B1**, indicating that the introduction of a methyl group at Cβ of the abstracting radical as in **B2** exerts a negligible effect on reactivity. This data are illustrated in the SI.

Conversely, branching at Cβ as in the case of **B3** determines a significant decrease in k_{XAT}, evidenced by the up to 1 order of magnitude decrease in reactivity observed in the reactions with **1**, **3**, **4**, **6**, and **7**, going from **B2** (or **B1**)[44] to **B3**, highlighting the important role exerted by radical sterics on these processes.

α-Aminoalkyl radicals generated from secondary and primary alkyl amines were evaluated next. Comparison between the k_{XAT} values measured for **B5** and **B2** shows a relatively small but noticeable decrease in reactivity (30−60%), which reflects the slightly decreased nucleophilicity of these systems.

An up to 2.3-fold decrease in k_{XAT} has been measured in the reactions with **4** and **7** going from **B5** to **B6**, and a progressive decrease has been measured in the reactions with **1** going from **B5** to **B6** and **B8** (k_{XAT} = 2.8 × 10^6, 1.8 × 10^6, and 1.3 × 10^6 M^{-1} s^{-1}, respectively). Although difficult to rationalize, these reactivity trends can be explained again in terms of the contribution of polar and steric effects.

https://doi.org/10.1021/jacsau.5c00920
JACS Au 2026, 6, 103−112

Where possible, comparison of the k_{XAT} values displayed in Figure 1c with those measured previously by Guo and co-workers[32] shows an excellent agreement, demonstrating the strong compatibility and complementarity between the LFP and TREPR techniques that taken together can expand the accessible reactivity range for bimolecular reactions involving radical intermediates. Accordingly, on the faster end the LFP technique with UV−vis detection allows the investigation of reactions of α-aminoalkyl radicals with tertiary iodides ($k_{XAT} \leq 5 \times 10^7$ M^{-1} s^{-1}), whereas, on the slower one, k_{XAT} values as low as 10^3 M^{-1} s^{-1} can be measured by employing the TREPR technique.

XAT Rate Constants and Substrate Effects for α-Aminobenzyl Radicals

Recent studies carried out by one of us have demonstrated that the steric and electronic features of α-aminoalkyl and α-aminobenzyl radicals can be finely tuned to enable selective reactivity in synthetic transformations.[45] For example, while **B1** efficiently promotes Giese addition of alkyl radicals generated from alkyl iodides to electron-poor olefins, this strategy fails with alkyl bromides due to intrinsically slower XAT, allowing direct Giese addition of **B1** to compete.[31] In contrast, **B4**, which was previously demonstrated to be unreactive toward Giese addition due to benzylic stabilization,[30] enables the recovery of XAT from alkyl bromides as the dominant pathway (Figure 2a).

The XAT reactivity of α-aminobenzyl radicals was recently questioned by Guo and co-workers, who reported negligible quenching ($k_{XAT} < 10^2$ M^{-1} s^{-1}) of alkyl iodides by radical **B4**.[32,45,46] On the basis of this experiment, they suggested that dehalogenation under photoredox conditions is not mediated by XAT but instead directly by the photocatalyst. Interestingly, observation of their original kinetic traces obtained by LFP with UV−vis detection shows a clear increase in the rate of decay with increasing substrate concentration, which in our opinion supports XAT reactivity.[45] As further supporting evidence, they conducted control reactions using a thermal persulfate/thiol system previously reported by one of us, which showed no product formation in the absence of light and photocatalyst.

In this work, we provide direct and conclusive evidence that α-aminobenzyl radicals are indeed capable of engaging in productive XAT with alkyl iodides. The rate of decay of the α-aminobenzyl radical visible absorption band was observed to increase with increasing alkyl iodide concentration (see Figure 2b and 2c for the kinetic traces relative to the reaction between **B4** and **4** and associated k_{obs} vs [**4**] plot, respectively), providing similar k_{XAT} values for the reactions of **B4**, **B7**, and **B9** with **4** ($k_{XAT} = 6.4 \times 10^4$, 5.7×10^4, and 5.2×10^4 M^{-1} s^{-1}, respectively). Even though these values are over 2 orders of magnitude lower than those measured for the corresponding reactions of α-aminoalkyl radicals (see Figure 1c above), in accordance with the well-known radical delocalization onto the phenyl ring displayed by benzylic radicals, they clearly confirm that reaction is occurring and thus the viability of XAT.

Moreover, through experiments carried out in the absence of a photoredox catalyst, employing electrophilic HAT reagents (triplet benzophenone (^{3}BP) and *t*-BuO•)[25,47] for the generation of **B4**, we confirm that α-aminobenzyl radicals enable XAT-based dehalogenation. As shown in Figure 2d, 390 nm photolysis of 4-iodo-*N*-Boc-piperidine **8** in the presence of methyl thioglycolate (20 mol %) and BP or $(t\text{-BuO})_2$ led to significant deiodination. Crucially, these results are in line with those obtained using a standard photoredox manifold with 4CzIPN as the photocatalyst. The similar result obtained with alkyl bromide (see SI, Section 6), albeit at a lower conversion, demonstrates the generality of α-aminobenzyl radical reactivity under photoredox-free conditions. Hence, correlating the isolated yield of a single reaction with the rate of a single elementary step such as XAT might be misleading, as the overall reaction efficiency could reflect a complex interplay of multiple steps, including undesired side processes (e.g., oxidation of the α-aminobenzyl radical), solubility effects, and amine-dependent oxidation, rather than a single rate constant alone.

Relevance of Polar Effects in XAT Reactions

A crucial aspect of the XAT reactivity of α-aminoalkyl radicals is the manifestation of polar and medium effects. To support these reactivity factors, we have performed a detailed computational analysis of the reactions of representative α-aminoalkyl and α-aminobenzyl radicals with alkyl iodides with a comparison to the corresponding all-carbon radical equivalents.

Initial benchmarking was conducted to select a reliable computational protocol, balancing accuracy and consistency with experimental rate data. Ultimately, we adopted a dual-level approach [M06-2X/def2TZVPP/CPCM(DMSO)//ωB97XD/def2SVP/CPCM(DMSO)] previously validated for related photochemical transformations.[48] More details are provided in the SI. While our method overestimates the absolute XAT barriers—particularly for delocalized benzylic radicals—it accurately reproduces relative trends and allows for mechanistic interpretations grounded in polar effects. Given the complexity of competing processes and the sensitivity of photochemical systems to multiple factors (e.g., solubility, side oxidation), our theoretical approach provides a reliable framework to dissect the intrinsic reactivity of α-amino radicals in XAT.

The XAT reactions of α-aminoalkyl, α-aminobenzyl, alkyl, and benzyl radicals with alkyl iodides feature the initial formation of a weakly bound prereaction complex held by dispersion forces, from where iodine abstraction takes place. The computed Gibbs free energies of complexation (ΔG_{cplx}), reaction (ΔG^0), and activation ($\Delta G^{\ddagger}$) show clear and consistent patterns. For the reactions of α-aminoalkyl and corresponding alkyl radicals, increasing substitution in the alkyl iodide lowers both ΔG^0 and $\Delta G^{\ddagger}$, in line with increased stabilization of the radical product.[48] However, a pronounced drop in reactivity was observed when moving from α-aminoalkyl to α-aminobenzyl radicals, with both ΔG^0 and $\Delta G^{\ddagger}$ increasing sharply. This is consistent with the experimental decrease in k_{XAT} observed in our transient spectroscopy studies. Notably, disubstituted and trisubstituted radicals within the same class (alkyl or benzyl) display comparable energetics, indicating a minimal steric influence on the transition state (see SI for more information).

When directly comparing α-aminoalkyl and α-aminobenzyl radicals (e.g., **B2** and **B4**) to their carbon-based analogues (e.g., **C2** and **C4**), key differences emerge. The α-amino radicals consistently show lower free energy barriers ($\Delta\Delta G^{\ddagger}$ = 2.5−9 kcal mol^{-1}) and more favorable thermodynamics ($\Delta G^0 < 0$) than their all-carbon counterparts, the reactions for which are typically thermoneutral to endergonic ($\Delta G^0 > 0$). Crucially, the complexation energies are nearly identical,

https://doi.org/10.1021/jacsau.5c00920
JACS Au 2026, 6, 103−112

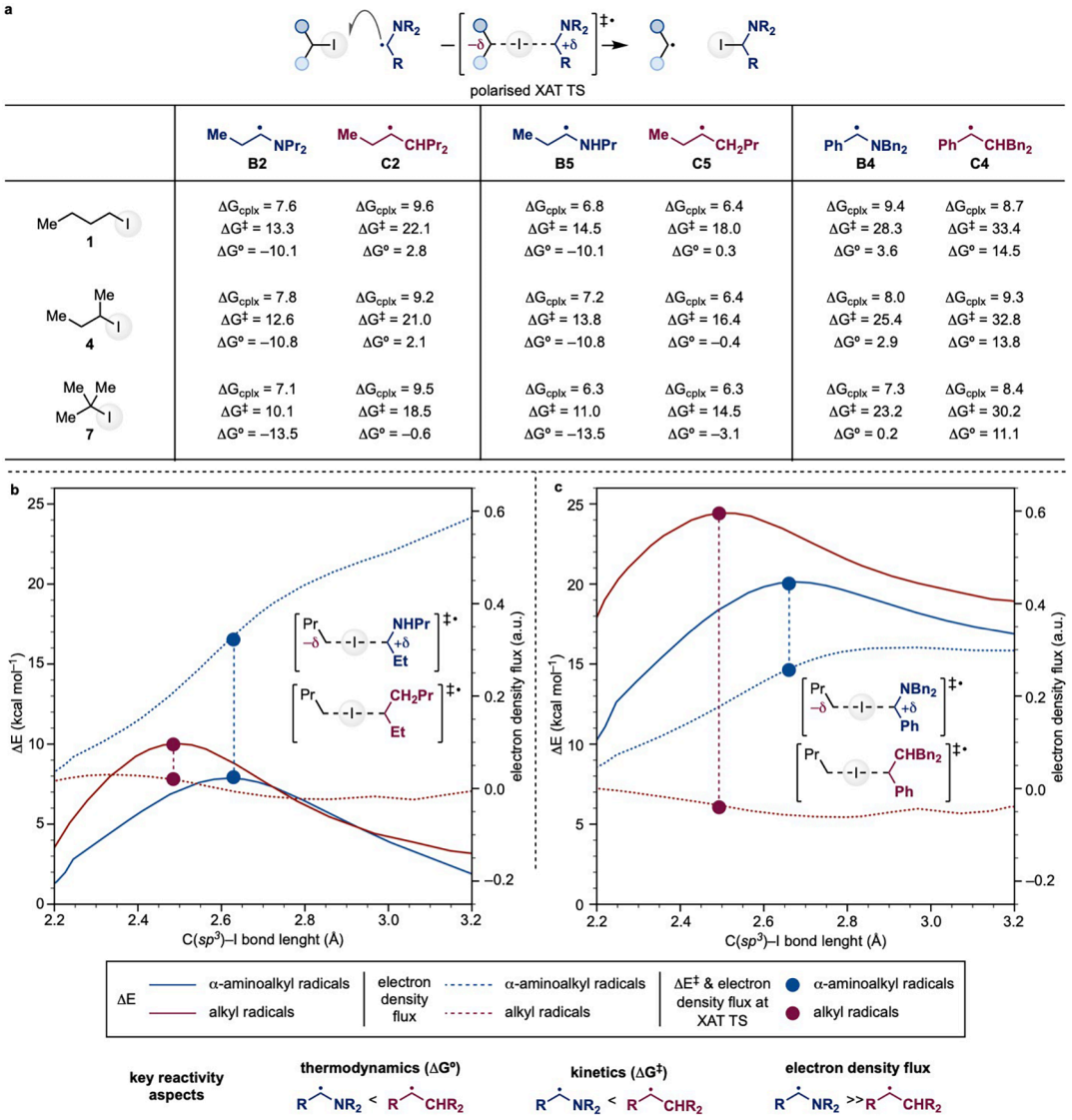

Figure 3. (a) Energetic parameters (in kcal mol^{-1}) for the XAT of α-aminoalkyl, α-aminobenzyl, alkyl, and benzyl radicals with iodides **1**, **4**, and **7**. (b) Analysis of the ΔE (solid line) and electron density flux (EDF, dotted line) along the XAT reaction profile between **B5** and **1** (blue) and **C5** and **1** (red). (c) Analysis of the ΔE (solid line) and electron density flux (dotted line) along the XAT reaction profile between **B4** and **1** (blue) and **C4** and **1** (red). The ΔE in (b) and (c) refers to the initial complex between **1** and radicals **B5**/**C5** and **B4**/**C4**.

highlighting that the observed differences originate from intrinsic electronic effects rather than association equilibria.

To elucidate the origin of the lower activation barriers observed for α-aminoalkyl radicals in XAT, we performed a detailed analysis of the charge redistribution along the intrinsic reaction coordinate (IRC) for representative model systems. Specifically, we investigated the electron density flux (EDF, which measures how much charge, i.e., electron density, moves from one molecular fragment to another along the reaction coordinate) as a function of the reaction coordinate for both α-aminoalkyl and α-aminobenzyl radicals and compared these to their all-carbon analogues. This analysis allows us to quantify the degree of polarity in the transition state and its evolution along the reaction pathway.

Figure 3b presents the free energy (ΔE) and EDF profiles (solid and dashed lines, respectively) for the reactions of radicals **B5** (blue lines) and **C5** (red lines) with 1-iodobutane **1**. For a detailed discussion, see the SI, sections 7.4 and 7.6. The former radical displays a marked increase in charge transfer along the reaction coordinate (indicated by the vertical dashed line at the transition state). In contrast, **C5** exhibits a nearly flat charge transfer profile, consistent with a nonpolar transition state. These observations are indicative, in the case of α-amino radical **B5**, of a mechanism driven by its enhanced nucleophilicity and ability to stabilize charge separation in the XAT transition state, highlighting the important role played by polar effects.

A similar pattern is observed for the benzylic systems in Figure 2c, comparing **B4** (blue lines) with **C4** (red lines), in their reactions with **1**. Although both systems show overall lower reactivity compared to their alkyl counterparts **B5** and **C5**, radical **B4** still exhibits appreciable charge transfer (EDF ≈ 0.3 au), whereas reaction of the corresponding all-carbon radical **C4** proceeds through a transition state that is essentially nonpolar. These results confirm that polar effects also play a key role in XAT reactions promoted by delocalized radicals.

These findings collectively support a model in which α-aminoalkyl and α-aminobenzyl radicals undergo XAT via a

https://doi.org/10.1021/jacsau.5c00920
JACS Au 2026, 6, 103−112

polar, charge-separated transition state that is stabilized by hyperconjugative overlap with the nitrogen lone pair. The absence of comparable charge redistribution in the all-carbon systems explains their consistently higher activation barriers and less favorable thermodynamics. Thus, the enhanced reactivity of α-amino radicals in XAT is not merely a result of thermodynamic driving force but also stems from fundamental differences in electronic structure and transition state stabilization.

Relevance of Medium Effects in XAT Reactions

Solvent polarity and H-bonding ability are known to exert a profound influence on radical reactions that proceed through polar transition states. In the context of XAT, this is especially relevant given the polar nature of the transition state when nucleophilic α-aminoalkyl radicals are involved, as shown by our computational analysis.

In their recent study, Guo and co-workers investigated solvent effects on XAT kinetics for the reaction of **B1** with cyclohexyl iodide **6**, by varying the composition of CH_3CN/H_2O solvent mixtures.[36] The authors observed a progressive decrease in k_{XAT} with increasing water content (from 4.2×10^6 to 3.1×10^6 M^{-1} s^{-1}, going from pure CH_3CN to CH_3CN + 15% H_2O), and therefore interpreted, on the basis of the associated increase in $E_T(30)$ value of the solvent mixture, as being inconsistent with a polar transition state, implying higher overall polarity. However, this interpretation overlooks the well-documented role of water and more generally hydrogen bond donating (HBD) solvents on radical reactivity.[37]

As established in previous kinetic investigations, HBD solvents such as water and fluorinated alcohols (e.g., HFIP) can significantly impact radical reactivity by forming H-bonds with the N-lone pair in amine substrates or radical species. This interaction leads to a buildup of positive charge that, with strong HBD solvents (and protonating agents), translates into a polarity reversal (Figure 4, left).[37] This means that the

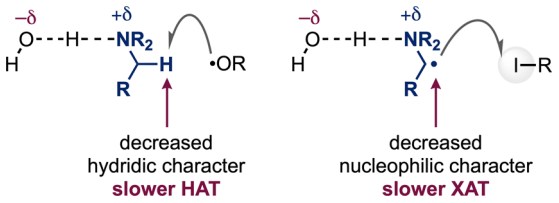

Figure 4. Effects of H-bonding interactions on HAT and XAT reactivity.

electron-donating character of the amine and the hydridic character of the α-C−H bonds are attenuated, reducing its ability to stabilize charge separation in the transition state. This has been thoroughly demonstrated in several HAT studies involving electrophilic radicals. For instance, in the reaction of CumylO• with **A1**, k_{HAT} decreased from 2.0×10^8 M^{-1} s^{-1} in CH_3CN to 1.47×10^8 and 9.2×10^7 M^{-1} s^{-1} upon addition of 1.0 and 4.7 M H_2O, respectively,[49] and significantly larger decreases in k_{HAT}, exceeding 3-orders of magnitude, were observed when employing stronger HBD solvents such as 2,2,2-trifluoroethanol (TFE).[50]

This HB interaction will also reduce the nucleophilicity of the α-aminoalkyl radical (Figure 4, right). Accordingly, the observed decrease in k_{XAT} upon increasing the water content in CH_3CN mixtures can be attributed to H-bonding between water and the nitrogen center of the α-aminoalkyl radical that determines transition state destabilization, decreasing XAT reactivity. Therefore, the data are entirely consistent with a polar transition state and in fact further support our mechanistic model in which the α-aminoalkyl radical's nucleophilic character plays a central role. Additional computational studies underscoring the influence of medium effects in this reaction are described in the Supporting Information, Section 7.7.

CONCLUSIONS

This study reinforces the validity of polar effects as a key reactivity factor in XAT from alkyl iodides to α-aminoalkyl radicals and directly confirms the reactivity of benzylic analogues under both photochemical and thermal conditions. While recent work has improved the accuracy of rate constants, broader mechanistic conclusions drawn from end point yields and incomplete kinetic models are not supported. Our findings clarify the mechanistic underpinnings of this widely adopted strategy and establish a quantitative framework for its continued application.

ASSOCIATED CONTENT

Supporting Information

The Supporting Information is available free of charge at https://pubs.acs.org/doi/10.1021/jacsau.5c00920.

Materials and methods (PDF)

Cartesian coordinates and energies (ZIP)

AUTHOR INFORMATION

Corresponding Authors

Michela Salamone − *Dipartimento di Scienze e Tecnologie Chimiche, Università "Tor Vergata", I-00133 Rome, Italy;* orcid.org/0000-0003-3501-3496; Email: michela.salamone@uniroma2.it

Massimo Bietti − *Dipartimento di Scienze e Tecnologie Chimiche, Università "Tor Vergata", I-00133 Rome, Italy;* orcid.org/0000-0001-5880-7614; Email: bietti@uniroma2.it

Daniele Leonori − *Institute of Organic Chemistry, RWTH Aachen University, 52056 Aachen, Germany;* orcid.org/0000-0002-7692-4504; Email: daniele.leonori@rwth-aachen.de

Authors

Jacopo Mancini − *Dipartimento di Scienze e Tecnologie Chimiche, Università "Tor Vergata", I-00133 Rome, Italy; Dipartimento di Chimica, Biologia e Biotecnologie, Università di Perugia, I-06123 Perugia, Italy*

Chiara Stavagna − *Institute of Organic Chemistry, RWTH Aachen University, 52056 Aachen, Germany;* orcid.org/0009-0000-4546-7841

Francesco Pileri − *Dipartimento di Scienze e Tecnologie Chimiche, Università "Tor Vergata", I-00133 Rome, Italy*

Giovanni Lonardi − *Institute of Organic Chemistry, RWTH Aachen University, 52056 Aachen, Germany*

Enrique M. Arpa − *Institute of Organic Chemistry, RWTH Aachen University, 52056 Aachen, Germany*

Marco Galeotti − *Dipartimento di Scienze e Tecnologie Chimiche, Università "Tor Vergata", I-00133 Rome, Italy; QBIS Research Group, Institut de Química Computacional i*

https://doi.org/10.1021/jacsau.5c00920
JACS Au 2026, 6, 103−112

Catàlisi (IQCC) and Departament de Química, Universitat de Girona, Girona E-17071 Catalonia, Spain

Sergio Sisti − *Dipartimento di Scienze e Tecnologie Chimiche, Università "Tor Vergata", I-00133 Rome, Italy*

Fabio Juliá − *Universidad de Murcia Edificio Pleiades-Vitalis, 30100 Murcia, Spain;* orcid.org/0000-0001-8903-4482

Complete contact information is available at: https://pubs.acs.org/10.1021/jacsau.5c00920

Author Contributions

[#]J. M. and C. S. contributed equally.

Notes

The authors declare no competing financial interest.

■ ACKNOWLEDGMENTS

G.L. and E.M.A. thank the Marie Curie Actions for their Fellowships (projects 101150093-BRADOCO and 101150311-NOZONE, respectively). The authors gratefully acknowledge the computing time provided to them at the NHR Center NHR4CES at RWTH Aachen University (project number p0021519). This is funded by the Federal Ministry of Education and Research and the state governments participating on the basis of the resolutions of the GWK for national high-performance computing at universities (www.nhr-verein.de/unsere-partner). The Dottorato di Interesse Nazionale (DIN) in Catalysis is gratefully acknowledged for a PhD grant to J.M.

■ REFERENCES

(1) Kim, H.; Lee, C. Visible-Light-Induced Photocatalytic Reductive Transformations of Organohalides. *Angew. Chem., Int. Ed.* **2012**, *51* (49), 12303−12306.

(2) Braslau, R.; Anderson, M. O. *Radicals in Organic Synthesis*; Wiley-VCH: Weinheim, Germany, 2002. DOI: 10.1002/1615-4169(200207)344:5<564::AID-ADSC564>3.0.CO;2-I.

(3) Wang, Z. Appel Reaction. In *Comprehensive Organic Name Reactions and Reagents*; Wiley, 2010; pp 95−99.

(4) Varenikov, A.; Shapiro, E.; Gandelman, M. Decarboxylative Halogenation of Organic Compounds. *Chem. Rev.* **2021**, *121* (1), 412−484.

(5) Agarwal, V.; Miles, Z. D.; Winter, J. M.; Eustáquio, A. S.; El Gamal, A. A.; Moore, B. S. Enzymatic Halogenation and Dehalogenation Reactions: Pervasive and Mechanistically Diverse. *Chem. Rev.* **2017**, *117* (8), 5619−5674.

(6) Sammes, P. G. Photochemistry of the C−X group. *Carbon-Halogen Bond* **1973**, 747−794.

(7) Nguyen, J. D.; D'Amato, E. M.; Narayanam, J. M. R.; Stephenson, C. R. J. Engaging unactivated alkyl, alkenyl and aryl iodides in visible-light-mediated free radical reactions. *Nat. Chem.* **2012**, *4* (10), 854−859.

(8) Cowper, N. G. W.; Chernowsky, C. P.; Williams, O. P.; Wickens, Z. K. Potent Reductants via Electron-Primed Photoredox Catalysis: Unlocking Aryl Chlorides for Radical Coupling. *J. Am. Chem. Soc.* **2020**, *142* (5), 2093−2099.

(9) Zhang, P.; Le, C. C.; MacMillan, D. W. C. Silyl Radical Activation of Alkyl Halides in Metallaphotoredox Catalysis: A Unique Pathway for Cross-Electrophile Coupling. *J. Am. Chem. Soc.* **2016**, *138* (26), 8084−8087.

(10) Le, C.; Chen, T. Q.; Liang, T.; Zhang, P.; MacMillan, D. W. C. A radical approach to the copper oxidative addition problem: Trifluoromethylation of bromoarenes. *Science* **2018**, *360* (6392), 1010−1014.

(11) Chan, A. Y.; Perry, I. B.; Bissonnette, N. B.; Buksh, B. F.; Edwards, G. A.; Frye, L. I.; Garry, O. L.; Lavagnino, M. N.; Li, B. X.; Liang, Y.; et al. Metallaphotoredox: The Merger of Photoredox and Transition Metal Catalysis. *Chem. Rev.* **2022**, *122* (2), 1485−1542.

(12) Danen, W. C.; Rose, K. A. Halogen abstraction studies. VI. Abstraction of bromine by phenyl radicals from C3-C8 cycloalkyl mono- and trans-1,2-dibromides. *Journal of Organic Chemistry* **1975**, *40* (5), 619−623.

(13) Tedder, J. M.; Walton, J. C. The importance of polarity and steric effects in determining the rate and orientation of free radical addition to olefins: Rules for determining the rate and preferred orientation. *Tetrahedron* **1980**, *36* (6), 701−707.

(14) Julia, F.; Constantin, T.; Leonori, D. Applications of Halogen-Atom Transfer (XAT) for the Generation of Carbon Radicals in Synthetic Photochemistry and Photocatalysis. *Chem. Rev.* **2022**, *122* (2), 2292−2352.

(15) Carlsson, D. J.; Ingold, K. U. Kinetics and rate constants for the reduction of alkyl halides by organotin hydrides. *J. Am. Chem. Soc.* **1968**, *90* (25), 7047−7055.

(16) Sidebottom, H.; Treacy, J. Reaction of methyl radicals with haloalkanes. *Int. J. Chem. Kinet.* **1984**, *16* (5), 579−590.

(17) Curran, D. P.; Jasperse, C. P.; Totleben, M. J. Approximate absolute rate constants for the reactions of tributyltin radicals with aryl and vinyl halides. *Journal of Organic Chemistry* **1991**, *56* (25), 7169−7172.

(18) Chatgilialoglu, C.; Ingold, K. U.; Scaiano, J. C.; Woynar, H. Absolute rate constants for some reactions involving triethylsilyl radicals in solution. *J. Am. Chem. Soc.* **1981**, *103* (11), 3231−3232.

(19) Baguley, P. A.; Walton, J. C. Flight from the Tyranny of Tin: The Quest for Practical Radical Sources Free from Metal Encumbrances. *Angew. Chem., Int. Ed. Engl.* **1998**, *37* (22), 3072−3082.

(20) Chatgilialoglu, C. Structural and Chemical Properties of Silyl Radicals. *Chem. Rev.* **1995**, *95* (5), 1229−1251.

(21) Sachidanandan, K.; Niu, B.; Laulhé, S. An Overview of α-Aminoalkyl Radical Mediated Halogen-Atom Transfer. *ChemCatChem.* **2023**, *15* (21), No. e202300860.

(22) Neff, R. K.; Su, Y. L.; Liu, S.; Rosado, M.; Zhang, X.; Doyle, M. P. Generation of Halomethyl Radicals by Halogen Atom Abstraction and Their Addition Reactions with Alkenes. *J. Am. Chem. Soc.* **2019**, *141* (42), 16643−16650.

(23) Su, Y.-L.; Tram, L.; Wherritt, D.; Arman, H.; Griffith, W. P.; Doyle, M. P. α-Amino Radical-Mediated Diverse Difunctionalization of Alkenes: Construction of C-C, C-N, and C-S Bonds. *ACS Catal.* **2020**, *10* (22), 13682−13687.

(24) Huang, J.-S.; Wang, Z.-H.; Li, X.-T.; Guo, S.-Y.; Jiang, X.-L.; Chen, Q.-A. Traceless Aminoalkyl Radical-Induced Halogen-Atom Transfer for Minisci Reactions. *Org. Lett.* **2025**, *27* (23), 6227−6232.

(25) Scaiano, J. C. Photochemical and free-radical processes in benzil-amine systems. Electron-donor properties of.alpha.-aminoalkyl radicals. *J. Phys. Chem.* **1981**, *85* (19), 2851−2855.

(26) DeLaive, P. J.; Foreman, T. K.; Giannotti, C.; Whitten, D. G. Photoinduced electron transfer reactions of transition-metal complexes with amines. Mechanistic studies of alternate pathways to back electron transfer. *J. Am. Chem. Soc.* **1980**, *102* (17), 5627−5631.

(27) Lalevée, J.; Gigmes, D.; Bertin, D.; Graff, B.; Allonas, X.; Fouassier, J. P. Comparative reactivity of aminyl and aminoalkyl radicals. *Chem. Phys. Lett.* **2007**, *438* (4), 346−350.

(28) Garwood, J. J. A.; Chen, A. D.; Nagib, D. A. Radical Polarity. *J. Am. Chem. Soc.* **2024**, *146* (41), 28034−28059.

(29) Ingold, K. U.; Lusztyk, J.; Scaiano, J. C. Absolute rate constants for the reactions of tributylgermyl and tributylstannyl radicals with carbonyl compounds, other unsaturated molecules, and organic halides. *J. Am. Chem. Soc.* **1984**, *106* (2), 343−348.

(30) Lalevee, J.; Graff, B.; Allonas, X.; Fouassier, J. P. Aminoalkyl radicals: direct observation and reactivity toward oxygen, 2,2,6,6-tetramethylpiperidine-N-oxyl, and methyl acrylate. *J. Phys. Chem. A* **2007**, *111* (30), 6991−6998.

(31) Lalevée, J.; Allonas, X.; Fouassier, J. P. Acrylate radicals: Direct observation and reactivity. *Chem. Phys. Lett.* **2005**, *415* (4), 287−290.

(32) Suo, W.; Qi, J.-Q.; Liu, J.; Sun, S.; Jiao, L.; Guo, X. Overestimated Halogen Atom Transfer Reactivity of α-Aminoalkyl Radicals. *J. Am. Chem. Soc.* **2024**, *146* (37), 25860−25869.
(33) Pischel, U.; Nau, W. M. Switch-Over in Photochemical Reaction Mechanism from Hydrogen Abstraction to Exciplex-Induced Quenching: Interaction of Triplet-Excited versus Singlet-Excited Acetone versus Cumyloxyl Radicals with Amines. *J. Am. Chem. Soc.* **2001**, *123* (40), 9727−9737.
(34) Salamone, M.; DiLabio, G. A.; Bietti, M. Hydrogen Atom Abstraction Selectivity in the Reactions of Alkylamines with the Benzyloxyl and Cumyloxyl Radicals. The Importance of Structure and of Substrate Radical Hydrogen Bonding. *J. Am. Chem. Soc.* **2011**, *133* (41), 16625−16634.
(35) Salamone, M.; Bietti, M. Reaction Pathways of Alkoxyl Radicals. The Role of Solvent Effects on C-C Bond Fragmentation and Hydrogen Atom Transfer Reactions. *Synlett* **2014**, *25*, 1803−1806.
(36) Abraham, M. H. Scales of solute hydrogen-bonding: their construction and application to physicochemical and biochemical processes. *Chem. Soc. Rev.* **1993**, *22* (2), 73−83.
(37) Bietti, M. Activation and Deactivation Strategies Promoted by Medium Effects for Selective Aliphatic C-H Bond Functionalization. *Angew. Chem., Int. Ed. Engl.* **2018**, *57* (51), 16618−16637.
(38) De Vleeschouwer, F.; Van Speybroeck, V.; Waroquier, M.; Geerlings, P.; De Proft, F. Electrophilicity and Nucleophilicity Index for Radicals. *Org. Lett.* **2007**, *9*, 2721−2724.
(39) Finn, M.; Friedline, R.; Suleman, N. K.; Wohl, C. J.; Tanko, J. M. Chemistry of the t-Butoxyl Radical: Evidence that Most Hydrogen Abstractions from Carbon are Entropy-Controlled. *J. Am. Chem. Soc.* **2004**, *126* (24), 7578−7584.
(40) Salamone, M.; Carboni, G.; Bietti, M. Fine Control over Site and Substrate Selectivity in Hydrogen Atom Transfer-Based Functionalization of Aliphatic C-H Bonds. *Journal of Organic Chemistry* **2016**, *81* (19), 9269−9278.
(41) Luo, Y.-R. *Comprehensive Handbook of Chemical Bond Energies*, 1st ed.; CRC Press, 2007. DOI: 10.1201/9781420007282.
(42) Martin, T.; Galeotti, M.; Salamone, M.; Liu, F.; Yu, Y.; Duan, M.; Houk, K. N.; Bietti, M. Deciphering Reactivity and Selectivity Patterns in Aliphatic C-H Bond Oxygenation of Cyclopentane and Cyclohexane Derivatives. *Journal of Organic Chemistry* **2021**, *86* (15), 9925−9937.
(43) Reichardt, C.; Welton, T. *Solvents and Solvent Effects in Organic Chemistry* **2010**, DOI: 10.1002/9783527632220.
(44) See SI for more information.
(45) Constantin, T.; Zanini, M.; Regni, A.; Sheikh, N. S.; Julia, F.; Leonori, D. Aminoalkyl radicals as halogen-atom transfer agents for activation of alkyl and aryl halides. *Science* **2020**, *367* (6481), 1021−1026.
(46) In this context, it is important to point out that analysis of the kinetic traces for the reaction between **B4** and cyclohexyl iodide monitored at 490 nm, as displayed in the SI of ref. 32 (Figure S24), shows a clear increase in the rate of decay of **B4** with increasing substrate concentration, suggesting the occurrence of a XAT reaction.
(47) Cohen, S. G.; Parola, A.; Parsons, G. H. Photoreduction by amines. *Chem. Rev.* **1973**, *73* (2), 141−161.
(48) Sanosa, N.; Peñín, B.; Sampedro, D.; Funes-Ardoiz, I. On the Mechanism of Halogen Atom Transfer from C-X Bonds to α-Aminoalkyl Radicals: A Computational Study. *Eur. J. Org. Chem.* **2022**, *2022* (34), No. e202200420.
(49) Bietti, M.; Salamone, M. Kinetic Solvent Effects on Hydrogen Abstraction Reactions from Carbon by the Cumyloxyl Radical. The Role of Hydrogen Bonding. *Org. Lett.* **2010**, *12* (16), 3654−3657.
(50) Salamone, M.; Ortega, V. B.; Martin, T.; Bietti, M. Hydrogen Atom Transfer from Alkanols and Alkanediols to the Cumyloxyl Radical: Kinetic Evaluation of the Contribution of α-C-H Activation and β-C-H Deactivation. *Journal of Organic Chemistry* **2018**, *83* (10), 5539−5545.

https://doi.org/10.1021/jacsau.5c00920
JACS Au 2026, 6, 103−112